nanomanufacturing

MDPI

Review

Graphene Nanofoam Based Nanomaterials: Manufacturing and Technical Prospects

Ayesha Kausar [1,2,3,*], Ishaq Ahmad [1,2,3], Tingkai Zhao [1,4], M. H. Eisa [5] and O. Aldaghri [5]

[1] NPU-NCP Joint International Research Center on Advanced Nanomaterials and Defects Engineering, Northwestern Polytechnical University, Xi'an 710072, China
[2] UNESCO-UNISA Africa Chair in Nanosciences/Nanotechnology, iThemba LABS, Somerset West 7129, South Africa
[3] NPU-NCP Joint International Research Center on Advanced Nanomaterials and Defects Engineering, National Centre for Physics, Islamabad 44000, Pakistan
[4] School of Materials Science & Engineering, Northwestern Polytechnical University, Xi'an 710072, China
[5] Department of Physics, College of Science, Imam Mohammad Ibn Saud Islamic University (IMSIU), Riyadh 13318, Saudi Arabia
* Correspondence: dr.ayeshakausar@yahoo.com

Abstract: This article fundamentally reviews progress in the design and manufacturing of three-dimensional (3D) graphene-based nanocomposites for technical applications. The 3D graphene nanostructures have been manufactured using techniques like the template method, chemical vapor deposition, sol-gel, freeze-drying, hydrothermal technique, and other approaches. The nanofoam has been reinforced in polymers to achieve superior structural, morphological, and physical characteristics of the ensuing polymer/graphene nanofoam nanocomposites. The polymer/graphene nanofoam nanocomposites have been manufactured using the approaches like direct template method, in situ technique, infiltration process, and other methods. The 3D nanofoam- and polymer-based nanostructures have shown high specific surface area, suppleness, electron transport, thermal conduction, mechanical resilience, and other physical properties. The technical applications of hierarchical graphene nanofoams have been observed in the fields of radiation shielding, solar cells, supercapacitors, fuel cells, and other applications.

Keywords: graphene; nanofoam; manufacturing; nanocomposite; solar cell; supercapacitor

check for updates

Citation: Kausar, A.; Ahmad, I.; Zhao, T.; Eisa, M.H.; Aldaghri, O. Graphene Nanofoam Based Nanomaterials: Manufacturing and Technical Prospects. *Nanomanufacturing* **2023**, *3*, 37–56. https://doi.org/10.3390/nanomanufacturing3010004

Academic Editor: Andres Castellanos-Gomez

Received: 2 January 2023
Revised: 12 January 2023
Accepted: 31 January 2023
Published: 1 February 2023

1. Introduction

Graphene is a two-dimensional nanocarbon nanomaterial with sp^2 hybridized carbon atoms [1]. It is a single-atom thick nanocarbon nano-allotrope. The van der Waals interactions may cause a nanosheet wrinkling effect [2,3]. Graphene has found potential applications in electronics, semiconductors, solar cells, and other technical fields [4]. In addition to two dimensional graphene, three dimensional (3D) graphene nanofoam has gained research attention [5]. The 3D graphene nanofoam or aerogel shows an excellent nano-porous structure and unique morphology. The graphene nanofoam not only exhibits the inherent properties of graphene nanosheet, but also reveals remarkable physical features [6]. Consequently, the 3D hierarchical nanofoam nanostructure possess high surface area, flexibility, robustness, porosity, and outstanding structural, mechanical, thermal, electrical, and other enhanced physical features [7,8]. Several approaches have been developed for the manufacture of graphene nanofoam such as template approach, chemical vapor deposition, freeze/supercritical drying, hydrothermal, sol-gel, and numerous other approaches [9–11]. The graphene nanofoam has been explored for the potential applications in the nanocomposites, electronics, supercapacitors, photovoltaics, batteries, energy, electronics, environment, and biomedical applications [12,13].

This state-of-the-art review presents advances in the design, manufacturing, and properties of 3D graphene nanofoam. Then, essential aspects of graphene nanofoam

based nanocomposites are discussed including the manufacturing approaches, essential properties, and application areas. The transformation of graphene nanosheet into 3D graphene nanofoam revealed remarkable structural and property innovations leading to promising application areas of the graphene nanofoam nanocomposite. Figure 1 shows the graphic of technical developments of graphene-to-graphene nanofoam and nanocomposite nanofoam for high-tech applications.

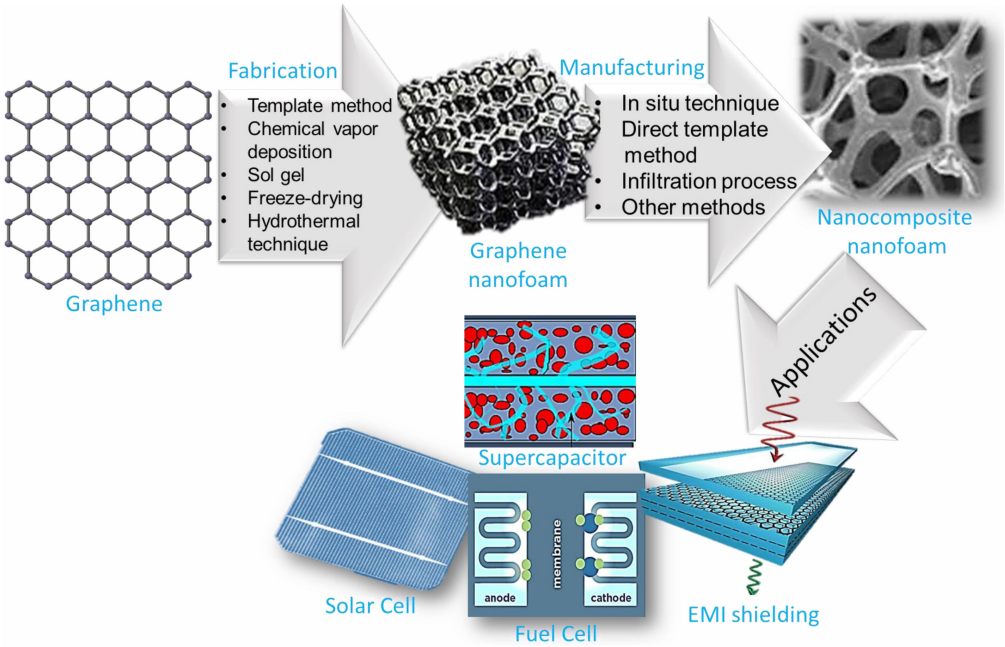

Figure 1. Schematic of technological developments of graphene-to-graphene nanofoam and nanocomposite nanofoam.

2. Nanofoam

Carbon nanofoam is a three-dimensional nano-allotrope of carbon [14,15]. In carbon nanofoam, the carbon atoms are arranged in a 3D hexagonal structure, which is often referred to as aerogel [16,17]. Initially, laser pulse technique was used to form the nanofoam using a carbon target in an inert atmosphere [18]. Carbon nanofoam exhibits high surface area and a transparent structure [19]. The three dimensional nanofoam has a C–C bond length of 5.6 Å [20]. The nanofoam usually possesses low density of ~2 mgcm^{-3}, and so it is lightweight [21]. Due to unpaired electrons, carbon nanofoam displays ferromagnetic properties below 90 K. Due to the magnetic properties, the carbon nanofoam revealed applications in spintronic devices and bio-imaging [22–24]. According to scanning/transmission electron microscopy, the nanofoam consists of woven forms of graphene nanosheets [25,26]. The periodic patterns have been observed in the three dimensional cross-linked nanostructures [27]. The simulation or computational studies have been performed to investigate the nanofoam nanostructures [28]. Furthermore, the carbon nanofoam has been applied in high-performance thermal insulation materials [29–31]. In addition, the three-dimensional nanofoam shows high electrical conductivity, thermal conductivity, and optical absorption [32,33]. The nanofoam displays a low dielectric constant, necessary for significant electrical properties [34]. The low dielectric constant and high charge transportation of these materials were found important for electronics/microelectronics applications [35,36]. The structure of carbon nanofoam has been modified through the inclusion of carbon nanoparticles (carbon nanotube or carbon nanofibers) in the three dimensional structure [37]. The modified nanofoam may lead to improved structural properties and high-tech applications.

3. 3D Graphene Nanofoam

Graphene is a unique two dimensional nanocarbon nanostructure [38,39]. It has a unique hexagonal arrangement of sp^2 hybrid carbon atoms with π bonding [40]. Owing to unique structure and superior physical properties, graphene presented potential for various advanced technical applications ranging from energy/electronics to biomedical devices [41–43]. The two dimensional graphene nanosheets can be arranged into a three dimensional nanostructures [44,45]. The 3D graphene is often referred as graphene nanofoam, graphene sponge, or graphene aerogel in the literature [46]. The three dimensional macro-assemblies of graphene have been developed due to van der Waals interactions between the nanosheets [47]. The three dimensional graphene nanofoam shows the intrinsic features of graphene and also novel physicochemical properties [48]. Consequently, the three dimensional graphene nanofoam possesses a large surface area, thermal transport, electrical conductivity, mechanical stability, porosity, and flexibility [49]. Graphene nanofoam has a high specific surface area of 1000 m^2g^{-1} [50]. The three-dimensional graphene nanofoam has high Young's moduli ~10^2 kPa [51]. Graphene nanofoam has been developed using graphene as well as graphene oxide.

Numerous manufacturing approaches have been applied for the formation of the three dimensional graphene [52]. Depending upon the fabrication strategy used, the graphene nanofoam may reveal different morphologies [53]. The template methods have been frequently used for the synthesis of graphene nanofoam [54]. Deng and co-workers [55] developed the three dimensional graphene on the nickel foam template via chemical vapor deposition technique (CVD). The graphene nanofoam has large surface area and mechanical robustness properties. Moreover, the graphene-nanofoam-based electrode showed high specific capacitance of 321 Fg^{-1} for high performance supercapacitor. Zhang et al. [56] proposed a route to graphene nanofoam using the template- and catalyst-based methods (Figure 2). The graphene nanofoam derived from the template method showed low density, high porosity, mechanical stability, and electrical conductivity [57].

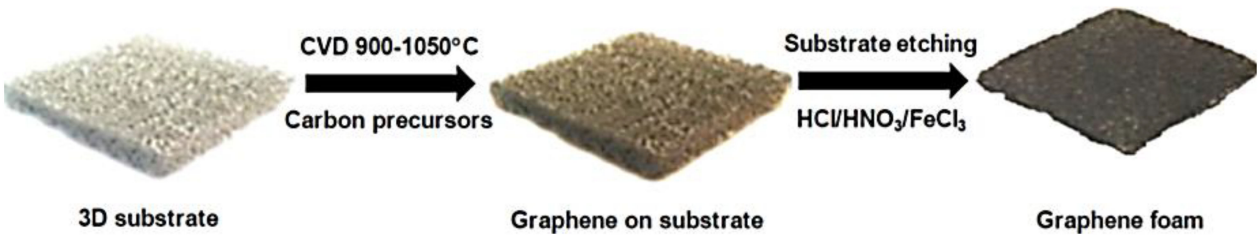

Figure 2. Schematic of synthesis of three dimensional graphene network through chemical vapor deposition. Reprinted with permission from Ref. [56]. 2022, MDPI.

Along with CVD, numerous other manufacturing methods have been used for the formation of graphene nanofoam [58]. Consequently, the freeze/supercritical drying approaches have been adopted to produce the 3D inter-linked graphene nanofoam [59,60]. The direct hydrothermal technique has also been applied for the formation of 3D graphene nanofoam with nanoparticles [61]. Zhang et al. [62] fabricated the 3D graphene nanofoam with titanium dioxide nanoparticles using the one-pot technique. The graphene nanofoam has efficient absorption properties [63]. Consequently, the nanofoam has been found useful for the adsorption-photo-electrocatalytic degradation of bisphenol A. The sol-gel technique was considered useful to prepare the 3D graphene oxide nanofoam [64]. The chemical cross-linking was observed due to reaction between hydroxyl, carbonyl, and epoxide functionalities of graphene oxide and the sol-gel precursor [65]. In this method, the heat/thermal treatment has been applied for the development of covalently linked 3D graphene structure [66]. During thermal treatment, the macro-assemblies of graphene oxide were reduced to graphene [67]. The sol-gel-derived graphene nanofoam revealed high surface area, porosity, electron mobility, and thermal conductivity properties [68,69]. The graphene nanofoam nanocomposites exhibited applications in catalysis, sensors, en-

ergy storage devices, absorbents, and biomedical fields [70]. Table 1 compares the various graphene nanofoam fabricated using numerous manufacturing approaches. All the mentioned methods have been efficiently used to prepare the high performance nanofoam.

Table 1. Essential properties of graphene nanofoam.

Nanofoam	Fabrication	Properties/Applications	Ref.
Graphene nanofoam	Chemical vapor deposition technique	Specific capacitance 321 Fg^{-1}	[55]
Graphene nanofoam	Template + catalyst method	Low density; high porosity; mechanical stability; electrical conductivity	[56]
Graphene nanofoam	Hydrothermal technique	Mechanical stability; electrical conductivity	[61]
Graphene nanofoam	One-pot technique	Absorption properties	[62]
Graphene nanofoam	Sol-gel technique; heat/thermal treatment	Chemical cross-linking; high surface area; porosity; electron mobility; thermal conductivity	[64,68,69]
Graphene nanofoam	Freeze-drying	1280 times higher elastic modulus than CVD nanofoam	[59]
Graphene nanofoam	Freeze-drying	Average pore size 70–100 µm	[71]
Graphene oxide foam	Freeze-drying	Compression strength; recovery after 300 compression cycles	[72]

4. Polymer/Graphene Nanofoam Nanocomposite

Numerous manufacturing approaches have been applied for the formation of 3D nanofoam nanoarchitectures [73]. The nanofoam-based nanocomposites displayed high surface area, low density, and high electronic, thermal, and mechanical characteristics [74]. Yao et al. [75] applied the simple one-pot surfactant-free technique to manufacture polymer/3D reduced graphene oxide nanofoam nanocomposites. The materials have been used for the supercapacitor electrodes. A significantly high specific capacitance of 952.85 Fg^{-1} was obtained. Tang et al. [76] fabricated the three dimensional reduced graphene oxide using the hydrothermal method. Then, the polyaniline/three-dimensional reduced graphene oxide nanocomposite was manufactured using the in situ technique. Figure 3 demonstrates the formation of the polyaniline/three-dimensional reduced graphene oxide nanocomposite. The nanomaterial was developed as supercapacitor electrode with high specific capacitance of 243 Fg^{-1}.

Wang et al. [77] manufactured the polyaniline/3D graphene oxide and reinforced in the epoxy matrix through the in situ oxidative polymerization. Figure 4 depicts the synthesis of epoxy and polyaniline/graphene oxide nanofoam derived nanocomposites. The graphene oxide nanofoam has been prepared using the freeze-drying method. The 3D graphene oxide nanofoam was reduced to the 3D graphene nanofoam. The in situ oxidative polymerization of aniline was performed on the 3D graphene nanofoam to form the nanocomposite. The resulting polyaniline/3D graphene nanofoam was reinforced in the epoxy matrix. The interface bonding between the polymer and nanofoam has been observed. The 0.39 wt.% nanofoam loading enhanced the electrical conductivity to 0.036 Scm^{-1}. Figure 5 shows the interfacial bonding mechanism for the formation of the nanocomposite. The π–π stacking interactions have been observed between the polyaniline and graphene structure.

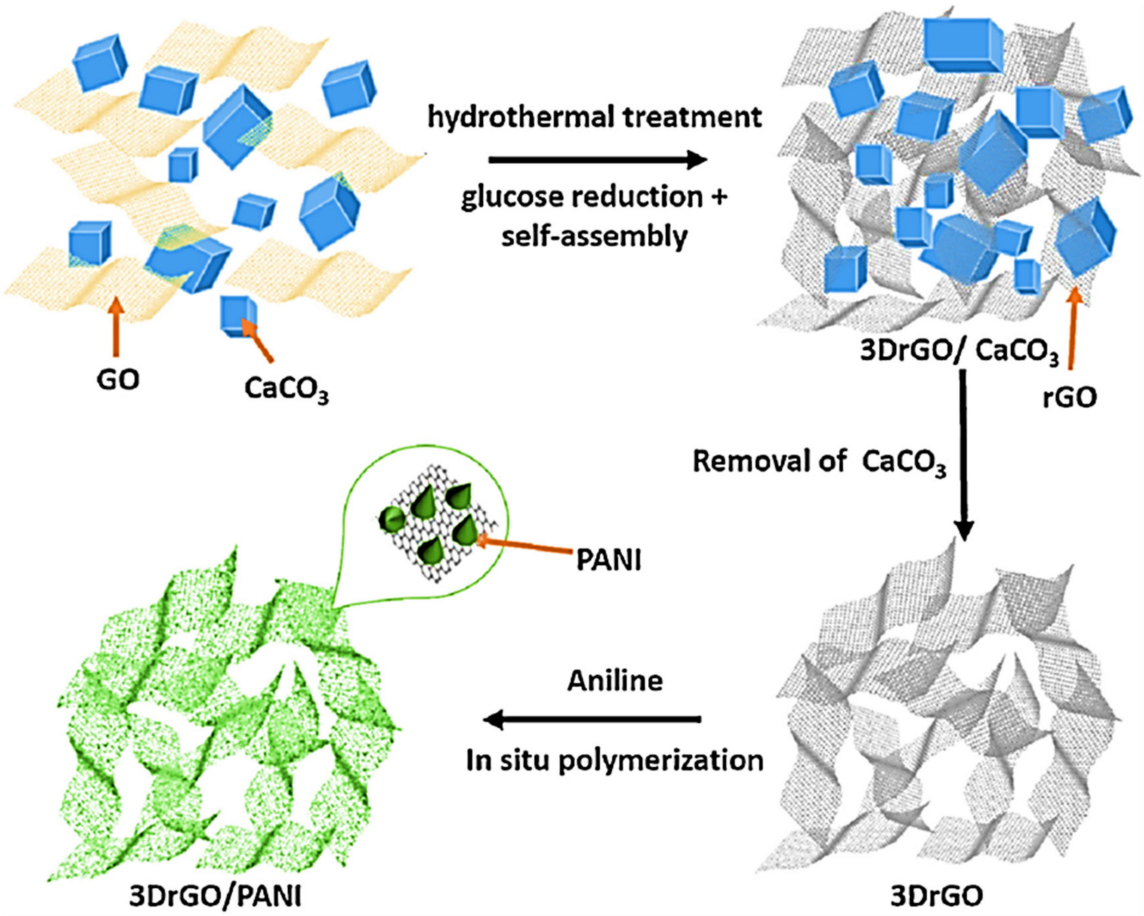

Figure 3. Preparation scheme of three dimensional reduced graphene oxide (3D-rGO) and three dimensional reduced graphene oxide/polyaniline (3D-rGO/PANI). GO = graphene oxide; PANI = polyaniline. Reprinted with permission from Ref. [76]. 2015, Elsevier.

Li et al. [78] performed the manufacturing of graphene nanofoam by hydrolytic condensation technique. The 3D polypyrrole/graphene oxide nanofoam was developed using the in situ route [79]. The 3D nanofoams were applied for oil and solvent adsorption. The sorption capacities were found to be high, >100 gg^{-1}, due to 3D covalent network formation in the nanofoams [80]. Salvatierra [81] reported on the preparation of polythiophene/graphene nanofoam nanocomposite through the one-pot in situ route.

Wang et al. [82] used the infiltration technique for the formation of the epoxy and graphene-nanofoam-based nanocomposite. Jia and co-workers [83] manufactured the graphene nanofoam reinforced epoxy derived nanocomposites using the infiltration method. The nanocomposite had high fracture toughness of 1.78 $MPa{\cdot}m^{1/2}$. Moreover, the 0.2 wt.% nanofoam loading revealed the electrical conductivity of 3 Scm^{-1}. Ormategui et.al. [84] proposed the epoxy and reduced graphene-oxide-nanofoam-based nanocomposite with superior electrical conductivity and mechanical properties.

Rinaldi [85] manufactured the poly(dimethyl siloxane) (PDMS) and graphene-nanofoam-based nanocomposite using direct template method. The PDMS/graphene-nanofoam-derived pressure sensor was developed, which detected pressure variations ~1 Pa. The nanocomposite sensing material had compressive stress ~10 kP. Zhao and co-workers [86] manufactured the poly(dimethyl siloxane) nanocomposites with graphene nanofoam and graphene sheet nanofillers. The nanocomposites were formed through the solution and infiltration routes. Figure 6 depicts the scanning/transmission electron microscopy images of the graphene nanofoam and graphene sheet. The graphene nanofoam had a three-dimensional structure, whereas the graphene sheet possesses a wrinkled structure. Figure 7 shows the thermal conductivity of neat PDMS and nanocomposite with graphene nanofoam and graphene

nanosheet. Neat PDMS revealed thermal conductivity of 0.19 $Wm^{-1}K^{-1}$. The graphene-nanofoam- and graphene-nanosheet-based nanocomposites had high thermal conductivity of 0.46 and 0.56 $Wm^{-1}K^{-1}$, respectively. The better graphene dispersion and inter-linked network formation led to better thermal conductivity and electron transportation properties.

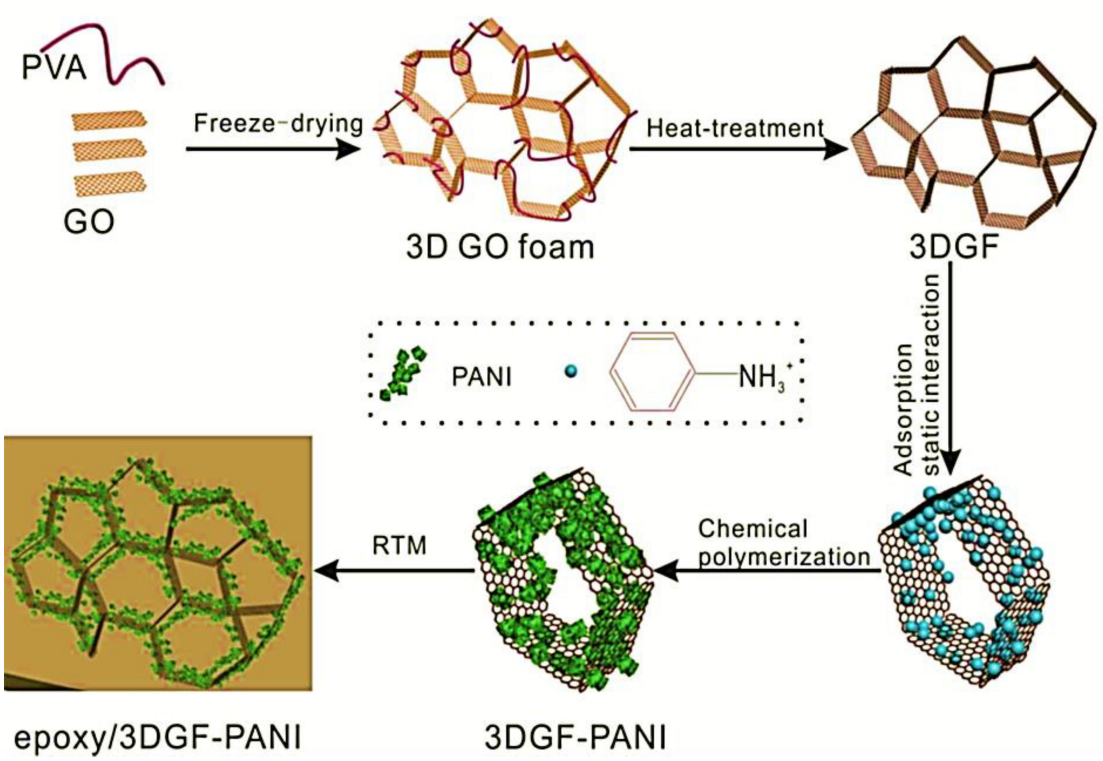

Figure 4. Schematic of preparation of three dimensional graphene oxide-polyaniline (3DGF-PANI) and epoxy/three dimensional graphene oxide-polyaniline (epoxy/3DGF-PANI) nanocomposite. Reprinted with permission from Ref. [77]. 2018, Elsevier.

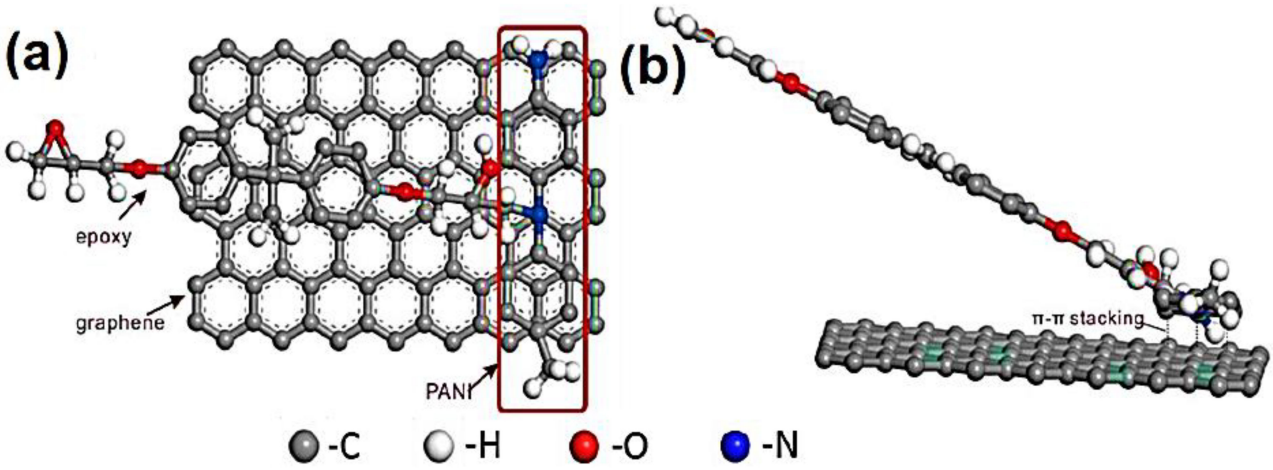

Figure 5. Schematic of proposed interfacial bonding mechanism (**a**) vertical view and (**b**) front view. Reprinted with permission from Ref. [77]. 2018, Elsevier.

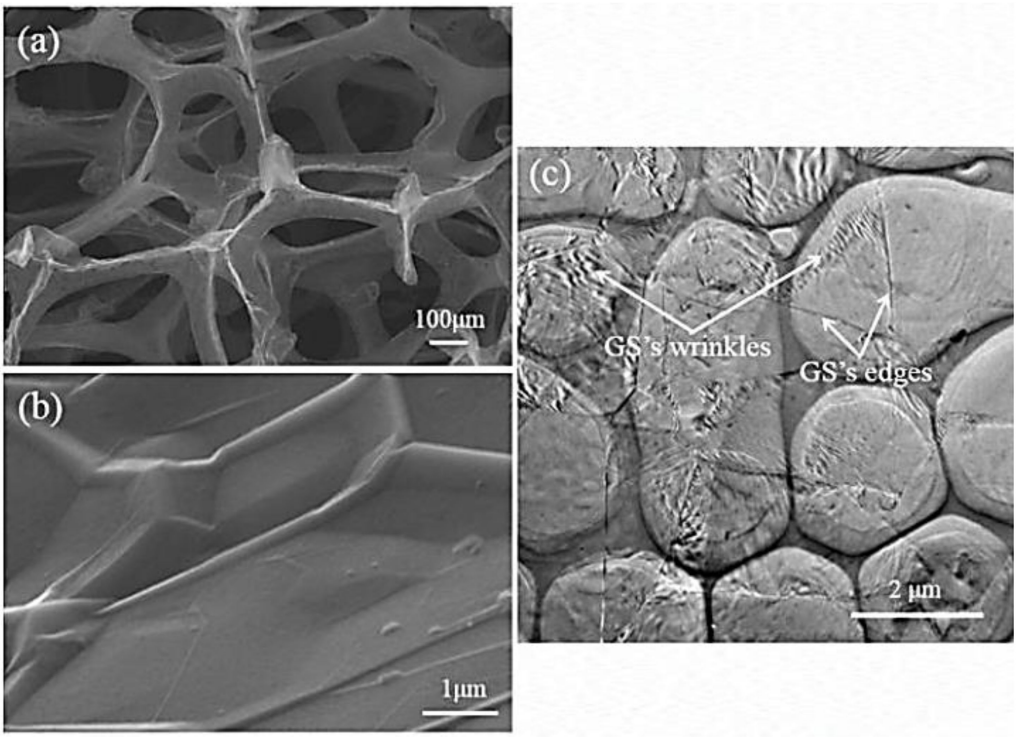

Figure 6. Scanning electron microscopy images of (**a**) graphene nanofoam; (**b**) graphene sheet; and (**c**) transmission electron microscopy image of graphene sheet. PDMS = poly(dimethyl siloxane); GF/PDMS = /poly(dimethyl siloxane); GS/PDMS = poly(dimethyl siloxane). Reprinted with permission from Ref. [86]. 2015, Elsevier.

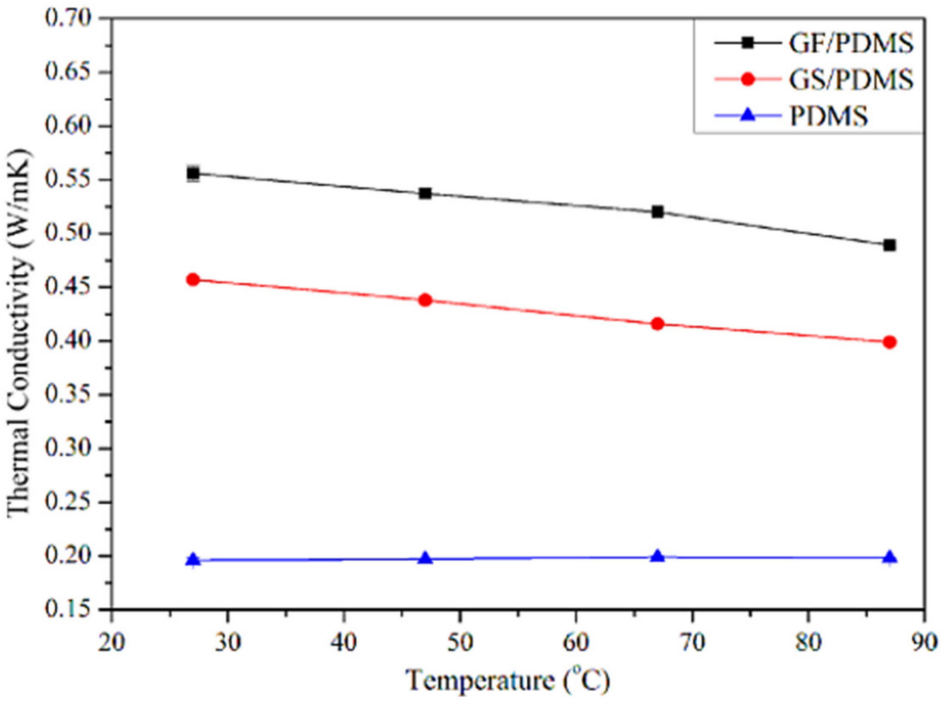

Figure 7. Thermal conductivity as a function of temperature. PDMS = poly(dimethyl siloxane); GF/PDMS = graphene nanofoam/poly(dimethyl siloxane); GS/PDMS = graphene sheet/poly(dimethyl siloxane). Reprinted with permission from Ref. [86]. 2015, Elsevier.

Jun et al. [87] manufactured the poly(dimethyl siloxane)/graphene nanofoam nanocomposites using the freeze-drying and infiltration methods. The small flake and large flake graphite nanosheets have been used to form the graphene nanofoam. Figure 8 demonstrates the manufacturing processes for the formation of graphene nanofoam by a freeze-drying technique. Later, the infiltration of PDMS resin through the nanofoam led to the formation of nanocomposite. Figure 9 depicts the in-plane electrical conductivity of the poly(dimethyl siloxane)/graphene nanofoam nanocomposites. The 1.9 wt.% large flake graphite led to high electrical conductivity of 102 Sm^{-1}, due to better dispersion and interconnecting matrix-nanofiller network formation.

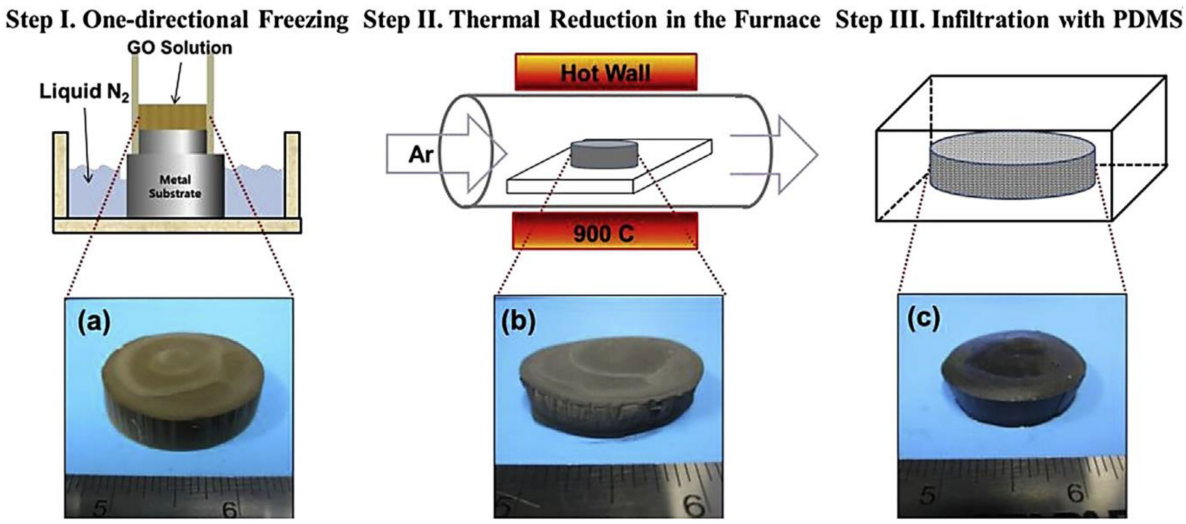

Figure 8. Schematic illustrating manufacturing procedure for (**a**) reduced graphene oxide nanofoam; (**b**) poly(dimethyl siloxane)/graphene nanofoam nanocomposite (**c**), and sliced slab of poly(dimethyl siloxane)/graphene nanofoam on probe fixture PDMS = poly(dimethyl siloxane); LFG = large flake graphite; SFG = small flake graphite. Reprinted with permission from Ref. [87]. 2015, Elsevier.

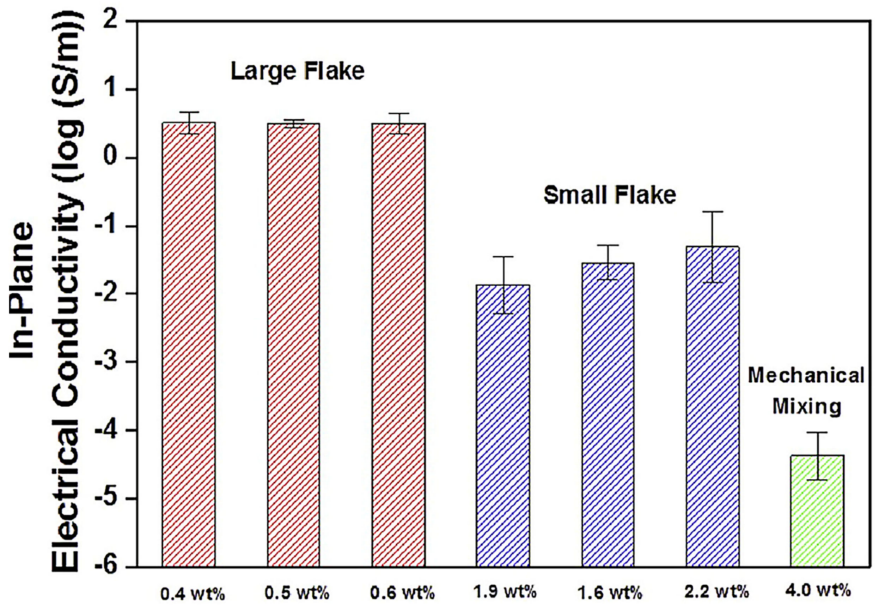

Figure 9. In-plane electrical conductivity of poly(dimethyl siloxane) nanocomposites produced from LFG and SFG, respectively. LFG = large flake graphite; SFG = small flake graphite. Reprinted with permission from Ref. [87]. 2015, Elsevier.

Zhao et al. [88] filled the PDMS matrix with the graphene nanofoam and carbon fiber fillers using high speed shearing and stirring techniques. The filler contents were varied up to 10 wt.%. The 10 wt.% filler addition enhanced the tensile strength and Young's modulus by 52% and 71%, respectively, relative to neat PDMS (Figure 10). The increase was credited to the strong interfacial bonding between the PDMS and the fillers. Moreover, the thermal conductivity of 0.55 Wm^{-1} K^{-1} was observed, that is, ~162% higher than the neat PDMS. Yuan and co-researchers [89] manufactured the polystyrene and graphene-nanofoam-based nanomaterials through the vacuum filtration technique. The polystyrene/graphene nanofoam was used to form the supercapacitor electrode and own large specific capacitance of 141–206 Fg^{-1}. Figure 11 shows the varying trend of specific capacitance as a function of current density for the graphene nanofoam nanocomposite.

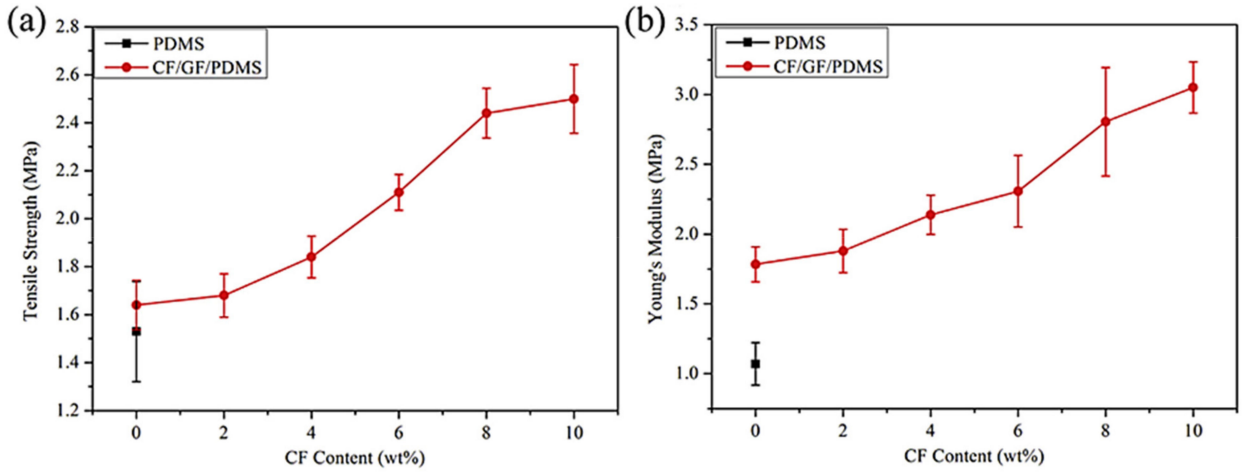

Figure 10. (**a**) Typical tensile strength and (**b**) Young's modulus of nanocomposite materials PDMS = poly(dimethyl siloxane); CF/GF/PDMS = carbon fiber/graphene nanofoam/poly(dimethyl siloxane). Reprinted with permission from Ref. [88]. 2016, Elsevier.

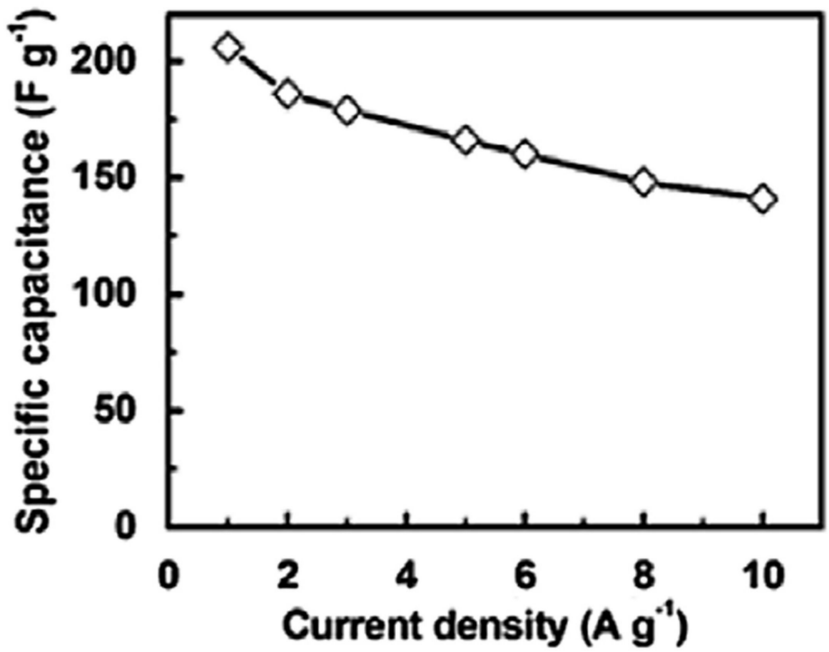

Figure 11. Specific capacitance vs. current density of graphene-nanofoam-based nanocomposite electrode. Reprinted with permission from Ref. [89]. 2014, Elsevier.

Gnanasekaran and co-workers [90] manufactured the polybutylene terephthalate/graphene nanofoam nanocomposite using the infiltration method. The nanomaterial was utilized for the printing of electrically conducting structures. Among other polymers, polyamide 6 has been composited with the graphene nanofoam through in situ polymerization [91]. The polyamide 6/graphene nanofoam nanocomposite had high thermal conductivity of 0.891 $Wm^{-1}K^{-1}$ [92]. Thus, various combinations of polymers with graphene nanofoam, graphene oxide nanofoam, and reduced graphene oxide nanofoam have been manufactured through facile routes. The nanofoam designs have been explored for the enhanced morphological, conducting, capacitance, thermal, and mechanical properties.

5. Significance of Polymer/Graphene Nanofoam Nanocomposite

The manufacturing and property exploration of the polymer/graphene nanofoam architectures have attracted considerable research attention in numerous technical fields [93,94]. Table 2 compares the essential polymer- and nanofoam-based nanomaterials with fabrication techniques, properties, and application areas. It has been observed that the conducting polymer-based nanocomposites revealed enhanced electrical conductivity properties for suitable applications. However, thermoplastic polymer/graphene nanofoam nanomaterials also revealed high performance and technical uses. Consequently, by manufacturing 3D graphene nanofoam instead of two-dimensional graphene nanostructures, high performance and industrial applications have been achieved.

Table 2. Specifications of polymer/graphene nanofoam nanocomposites.

Polymer	Nanofoam	Fabrication	Properties/Applications	Ref.
Polymer	3D reduced graphene oxide nanofoam	One-pot surfactant-free technique	Supercapacitor; specific capacitance 952.85 Fg^{-1}	[75]
Polyaniline	3D reduced graphene oxide	Hydrothermal method; in situ technique	Supercapacitor; specific capacitance 243 Fg^{-1}	[76]
Polyaniline	3D graphene oxide	Freeze-drying; In situ oxidative polymerization	π-π stacking interactions; electrical conductivity 0.036 Scm^{-1}	[77]
Polypyrrole	Graphene oxide nanofoam	Hydrolytic condensation; in situ route	Oil/solvent adsorption; sorption capacities >100 gg^{-1}	[76,78]
Polythiophene/	Graphene nanofoam	In situ route	Electrical conductivity	[81]
Epoxy	Graphene nanofoam	Infiltration method	Fracture toughness 1.78 $MPa{\cdot}m^{1/2}$; electrical conductivity 3 Scm^{-1}	[83]
Poly(dimethyl siloxane)	Graphene nanofoam	Direct template method	Pressure sensor; pressure variations ~1 Pa; compressive stress ~10 kP	[85]
Poly(dimethyl siloxane)	Graphene nanofoam	Solution and infiltration route	Thermal conductivity 0.56 $Wm^{-1}K^{-1}$	[86]
Poly(dimethyl siloxane)	Graphene nanofoam	Freeze-drying; infiltration methods	Electrical conductivity 102 Sm^{-1}	[87]
Poly(dimethyl siloxane)	Graphene nanofoam	High speed shearing and stirring techniques	Increase in tensile strength 52%; Young's modulus 71%; thermal conductivity 0.55 Wm^{-1} K^{-1} i.e., increase by 162%	[88]

Table 2. *Cont.*

Polymer	Nanofoam	Fabrication	Properties/Applications	Ref.
Polystyrene	Graphene nanofoam	Vacuum filtration technique	Supercapacitor; specific capacitance 141–206 Fg^{-1}	[89]
Polybutylene terephthalate	Graphene nanofoam	Infiltration method.	Thermal conductivity 0.891 $Wm^{-1}K^{-1}$	[90]
Poly(3,4-ethylenedioxythiophene): poly(styrenesulfonate)	Graphene nanofoam	Drop coating technique	High porosity 98.8%; ultralow density ~18.2 × 10^{-3} g/cm^3; EMI shielding effectiveness 91.9 dB; electrical conductivity 43.2 Scm^{-1}	[95]
Poly(vinylidene fluoride)	Graphene nanofoam	Hot pressing technique	EMI shielding effectiveness ~20 dB; electrical conductivity 10^{-4} S m^{-1}	[96]
Polyurethane	Graphene nanofoam	Hydrothermal method	EMI shielding effectiveness 969–1578 $dBcm^2g^{-1}$	[97]
Polymer	Graphene nanofoam	CVD; spin coating techniques	Dye sensitized solar cells; AM 1.5 illumination	[98]
Polymer	Graphene nanofoam	Solution/ coating	Power conversion efficiency 6.58%; short-circuit current density 15.4 $mAcm^{-2}$; dye absorption efficiency ~1.28 × 10^{-7} mol cm^{-2}	[99]
Polypyrrole	Graphene nanofoam	Solution dispersion; chemical/hydrothermal reduction routes	Specific capacitance 253–520 Fg^{-1}	[100]
Polyaniline	Graphene nanofoam	One-step electrochemical deposition	Specific capacitance 751 Fg^{-1}	[101]
Poly(methyl methacrylate) nanofoaming	Graphene	Thermal annealing method	Polymer electrolyte membrane fuel cell; high power density ∼967 mW cm^{-2}	[102]

Consequently, significant technical application areas of the polymer/3D graphene nanofoam nanomaterials have been discovered [94]. The electromagnetic pollution, due to intensive use of electronic devices, has caused serious environmental issues [103]. In this regard, the electromagnetic interference (EMI) shielding nanocomposites were manufactured through the three dimensional graphene nanofoams [104]. Owing to high electrical conductivity, the graphene-nanofoam-based nanocomposites revealed fine EMI shielding performance. The graphene-nanofoam-based nanocomposites possess high durability, flexibility, and radiation protection features [105]. Such materials have been found very useful in the aerospace sector for radiation shielding [106]. Important research attempts have been found on the conducting polymer/graphene nanofoam nanocomposites for EMI shielding applications [107,108]. Wu et al. [95] manufactured the ultralight poly(3,4-ethylenedioxythiophene):poly(styrenesulfonate)/graphene nanocomposite nanofoam using the drop coating technique. This method resulted in enhanced wettability and interfacial interactions between the poly(3,4-ethylenedioxythiophene):poly(styrenesulfonate) matrix and graphene nanofoam. The nanocomposite nanofoam revealed high porosity (98.8%) and ultralow density ~18.2 × 10^{-3} g/cm^3. Due to a finely interlinked 3D network structure, high electrical conductivity of 43.2 Scm^{-1} was obtained. Consequently, the nanocomposite nanofoam revealed significantly high EMI shielding effectiveness of 91.9 dB. In addition, thermoplastic polymer/graphene nanofoam has been developed for

EMI shielding applications [109]. Eswaraiah et al. [96] manufactured the poly(vinylidene fluoride)/graphene nanofoam nanomaterials using the hot pressing technique with a foaming agent. Due to fine compatibility between polymer–graphene nanofoam and conducting network formation, the electrical conductivity of nanomaterial (10^{-4} S m^{-1}) was found to be higher than the neat polymer (10^{-16} S m^{-1}). Consequently, the 0.5 wt.% graphene nanofoam contents led to EMI shielding effectiveness of ~20 dB in X-band (8–12 GHz). Furthermore, the polyurethane and graphene nanofoam nanocomposites have been manufactured through the hydrothermal method [97]. Due to superconductivity features, the polyurethane/graphene nanofoam nanocomposites own high EMI shielding effectiveness of 969–1578 dBcm^{2}g^{-1}. Future research attempts have been found desirable for lightweight high-performance polymer/graphene-nanofoam-based EMI shielding materials for X-band. Additionally, the mechanism of EMI shielding in these nanomaterials need to be explored in the future.

Another important application of 3D graphene nanofoam has been observed in photovoltaics [110]. By converting the 2D graphene to 3D graphene nanofoam network, remarkable solar cell performance has been observed for solar cells [111]. In this regard, graphene-nanofoam-based dye sensitized solar cells (DSSC) have been developed and analyzed for environmental stability, toxicity, cost-effective, and commercial uses. Lee et al. [98] designed the 3D nanofoam using CVD and spin coating techniques on the polymer/nickel. The photovoltaic performance of DSSC was measured with AM 1.5 illumination (100 mW cm^2). Tang et al. [99] manufactured DSSC using graphene nanofoam and CVD system. The graphene nanofoam was applied as the photoanode to enhance the photovoltaic functioning (Figure 12 and Table 3). Inclusion of 1 wt.% graphene nanofoam resulted in high power conversion efficiency and short-circuit current density of 6.58% and 15.4 mAcm^{-2}, respectively. The graphene-nanofoam-based material had high dye absorption efficiency of ~1.28 × 10^{-7} mol cm^{-2}. The nanomaterial depicted competent solar cell efficiency, dye absorption, and electrode lifetime. However, limited research attempts have been seen in the field of polymer/graphene-nanofoam-based DSSC and need to be further explored.

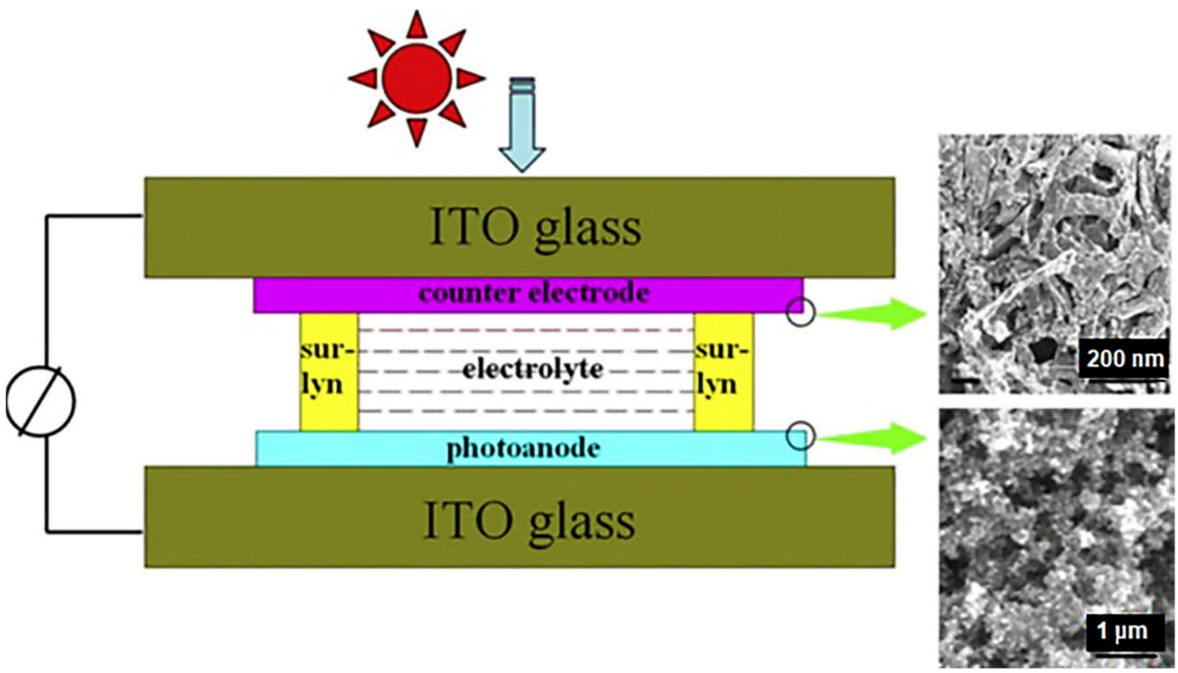

Figure 12. DSSC with graphene-nanofoam-based photoanode. DSSC = dye sensitized solar cell. Reprinted with permission from Ref. [99]. 2013, Elsevier.

Table 3. Results of photovoltaic properties and dye loading of the DSSC with varied photoanodes. DSSC = dye sensitized solar cell. Reprinted with permission from Ref. [99]. 2013, Elsevier.

Photoanode	Short Circuit Current Density (Jsc) ($mAcm^{-2}$)	Photovoltaic Bias (Voc) (mV)	Fill Factor (FF) (%)	Efficiency η (%)	Absorbed Dye ($\times 10^{-7}$mol cm^{-2})
3D graphene nanofoam 0.5 wt.%	13.6	671	63.4	5.79	1.03
3D graphene nanofoam 1 wt.%	15.4	673	63.5	6.58	1.15
3D graphene nanofoam 2 wt.%	11	674	63.2	6.01	1.28

Supercapacitors are an efficient energy storage device exhibiting ultrahigh capacitance, power density, and long cycle life [112]. The supercapacitor materials have been researched for low cost, high specific surface area, mechanical robustness, and chemical stability properties [113,114]. Especially, graphene is an emerging carbon material used in the field of energy storage. The graphene nanofiller has been reinforced in the polymers for enhanced supercapacitance features [115]. For supercapacitors, the 3D graphene-nanofoam-based electrodes have also been used [116]. The polypyrrole/3D graphene nanofoam derived electrodes had elevated specific capacitance of ~300 F/g [117]. Graphene nanofoam exposed capacitance of ≥95% over 1000 galvanostatic charge/discharge cycles. Moreover, the epoxy/graphene nanofoam with nanoparticles have been used to form the supercapacitor electrode capacitance [118,119]. The supercapacitor electrode showed capacitance of 38 $mFcm^{-2}$ and current density of 0.67 $mAcm^{-2}$. The resulting supercapacitors possess high power efficiency and long lifetime [120]. Ye et al. [100] formed the 3D polypyrrole/graphene nanofoam using solution dispersion and chemical/hydrothermal reduction routes. The π–π stacking interactions were observed between the polypyrrole and graphene nanofoam. The nanocomposite nanofoam possess high specific surface areas and uniform porosity. The 3D interlinked hierarchically porous nanostructure led to high specific capacitance of 253–520 Fg^{-1} and excellent cycling stability [121]. Yu et al. [101] prepared the 3D polyaniline/graphene nanofoam using one-step electrochemical deposition technique. The highly ordered 3D nanostructure of polyaniline/graphene nanofoam electrode had high specific capacitance of 751 Fg^{-1} and capacitance retention of 98.2% after 1000 charging/discharging cycles. Future research attempts must focus the design of chemically/thermally stable conducting polymer/graphene nanofoam and use of green nanomaterials for advanced supercapacitors for commercial applications.

Graphene nanofoam has also been applied in electronics such as batteries, sensors, etc. [122,123]. To advance the existing lithium–sulfur batteries for the current energy storage marketplace, it has been found essential to increase the electrochemical stability of the sulfur electrodes [124]. In this regard, graphene nanofoam has been designed as a current collector for the lithium–sulfur battery cathode. The graphene nanofoam may develop tortuous conducting network to enhance the conductivity of sulfur cathodes. CVD technique has been used to form graphene-nanofoam-based electrodes for lithium–sulfur batteries [125]. Few attempts have also been observed on the graphene-nanofoam-based strain sensors [126]. Electron transportation through these sensors has been analyzed [127]. The potential application of graphene nanofoam in straintronics may result in further advances in this field [128]. Nevertheless, few polymer/graphene-nanofoam-derived nanomaterials have been applied for electronics, and further efforts are needed to explore the full potential of these materials in this application.

For fuel cell applications, latest advances have revealed the use of graphene-based nanomaterials in the bipolar plates, electrodes, and electrolytes [129]. In this regard, the novel graphene-based nanomaterials and related structure-property relationships have been explored. Accordingly, the graphene nanofoam has been applied as catalyst supports [130]. Especially, graphene nanofoam has been used as anode electrode for the microbial fuel cell [131]. High power density of 427.0 W/m^3 of fuel cell was observed.

Research efforts have been performed for improving the operational stability and lifetime of the polymer electrolyte membrane fuel cell (PEMFC) [132]. Nevertheless, the corrosion of metal bipolar plates has been observed as a major challenge in PEMFC, which may lead to low fuel cell efficiency and durability [133]. Sim et al. [102] designed the 3D nanostructure based on the poly(methyl methacrylate)/multilayer graphene using the rapid thermal annealing method. The 3D poly(methyl methacrylate)/graphene nanofoam was used to form the bipolar plate for fuel cell. The resulting PEMFC revealed significantly high power density of $\sim$967 mW cm^{-2} at cell potential of 0.5 V. Moreover, the interfacial contact resistance of 9.3 mΩ cm^2 was observed at 10.1 kgf cm^{-2}. Future efforts on manufacturing the novel polymer/graphene nanofoam designs may help to overcome the limitations of present PEMFC systems and to further enhance the efficiency of these energy conversion systems.

In future, the graphene-nanofoam-derived nanofibers can be developed for various unexplored technical application areas [134–136]. Moreover, large-scale production of polymer/graphene nanofoam materials need to be focused on in the future. In addition, the polymer/graphene nanofoams nanocomposites need to be explored in numerous uncovered areas like separation/purification applications, dye adsorption, oil–water separation, tissue engineering, and other biomedical fields [137–139]. Here, the choice of appropriate fabrication technique, in addition to the graphene-nanofoam-derived nanocomposite design led to high-tech applications.

6. Conclusions

The two-dimensional graphene has been applied to manufacture the 3D network structure of graphene nanofoam. The intrinsic features of graphene have been embodied in the graphene nanofoam architecture along with several exceptional properties of 3D nanostructure. Therefore, the graphene nanofoam show numerous beneficial features, relative to the neat graphene. The graphene nanofoam was manufactured using efficient techniques. An important use of graphene nanofoam has been observed in nanocomposite manufacturing. Here, the developments in design, features, and application areas of polymer and graphene nanofoam nanocomposite have been discussed. The graphene-nanofoam-derived nanocomposites, obtained through facile manufacturing techniques, led to high performance advanced uses. Graphene nanofoam has been found as a true wonder material that promises much in a variety of applications. Different facile methods have been discovered for the synthesis of graphene nanofoam and related nanomaterials, leading to viability and practicalities for the different practical relevance. Consequently, the modification of graphene-to-graphene nanofoam and polymer/graphene nanofoam has a marked impact in manifold applications including radiation shielding, energy storage/production devices, and electronics. Consequently, the current state-of-the-art graphene nanofoam research revolves around the EMI shielding, energy, and electronics fields. The development of 3D graphene nanostructures offers large surface area, porosity, electron transportation, charge passage, specific capacitance, current density, and radiation shielding effectiveness. Here, the interactions between the polymers and 3D graphene nanofoam are essential to improve the nanocomposite performance. Furthermore, the precise control over the pore size/distribution, flexibility, morphology, conductivity, and mechanical/chemical stability, and structure–property relationships of the materials may lead to future high-tech potential of unique graphene-nanofoam-based nanocomposites.

Author Contributions: Conceptualization, A.K.; data curation, A.K.; writing of original draft preparation, A.K.; Review and editing, A.K., I.A., T.Z., M.H.E. and O.A. All authors have read and agreed to the published version of the manuscript.

Funding: This research received no external funding.

Data Availability Statement: Not applicable.

Conflicts of Interest: The authors declare no conflict of interest.

References

1. Xiong, Z.; Marconnet, A.; Ruan, X. Unconventional and Dynamically Anisotropic Thermal Conductivity in Compressed Flexible Graphene Foams. *ACS Appl. Mater. Interfaces* **2022**, *14*, 48960–48966. [CrossRef] [PubMed]
2. Mubarik, S.; Qureshi, N.; Sattar, Z.; Shaheen, A.; Kalsoom, A.; Imran, M.; Hanif, F. Synthetic approach to rice waste-derived carbon-based nanomaterials and their applications. *Nanomanufacturing* **2021**, *1*, 109–159. [CrossRef]
3. Trout, C.J.; Kumpf, P.; Sipps, K.; Griepenburg, J.C.; O'Malley, S.M. The Influence of Alkanethiols on the Production of Hydrophobic Gold Nanoparticles via Pulsed Laser Ablation in Liquids. *Nanomanufacturing* **2021**, *1*, 9. [CrossRef]
4. Gao, J.; Li, Y.; Yu, X.; Ma, Y. Graphdiyne reinforced multifunctional Cu/Ni bimetallic Phosphides-Graphdiyne hybrid nanostructure as high performance electrocatalyst for water splitting. *J. Colloid Interface Sci.* **2022**, *628*, 508–518. [CrossRef] [PubMed]
5. Kausar, A. *Graphene to Polymer/Graphene Nanocomposites: Emerging Research and Opportunities*; Elsevier: Amsterdam, The Netherlands, 2021.
6. Yin, S.; Niu, Z.; Chen, X. Assembly of graphene sheets into 3D macroscopic structures. *Small* **2012**, *8*, 2458–2463. [CrossRef]
7. Gao, H.; Duan, H. 2D and 3D graphene materials: Preparation and bioelectrochemical applications. *Biosens. Bioelectron.* **2015**, *65*, 404–419. [CrossRef] [PubMed]
8. Zhu, C.; Han, T.Y.-J.; Duoss, E.B.; Golobic, A.M.; Kuntz, J.D.; Spadaccini, C.M.; Worsley, M.A. Highly compressible 3D periodic graphene aerogel microlattices. *Nat. Commun.* **2015**, *6*, 6962. [CrossRef]
9. Su, D. Macroporous 'bubble'graphene film via template-directed ordered-assembly for high rate supercapacitors. *Chem. Commun.* **2012**, *48*, 7149–7151.
10. Chen, Z.; Ren, W.; Gao, L.; Liu, B.; Pei, S.; Cheng, H.-M. Three-dimensional flexible and conductive interconnected graphene networks grown by chemical vapour deposition. *Nat. Mater.* **2011**, *10*, 424. [CrossRef]
11. Cao, X.; Shi, Y.; Shi, W.; Lu, G.; Huang, X.; Yan, Q.; Zhang, Q.; Zhang, H. Preparation of novel 3D graphene networks for supercapacitor applications. *Small* **2011**, *7*, 3163–3168. [CrossRef]
12. Choi, B.G.; Yang, M.; Hong, W.H.; Choi, J.W.; Huh, Y.S. 3D macroporous graphene frameworks for supercapacitors with high energy and power densities. *ACS Nano* **2012**, *6*, 4020–4028. [CrossRef] [PubMed]
13. Chen, W.; Li, S.; Chen, C.; Yan, L. Self-assembly and embedding of nanoparticles by in situ reduced graphene for preparation of a 3D graphene/nanoparticle aerogel. *Adv. Mater.* **2011**, *23*, 5679–5683. [CrossRef]
14. Liu, Y.; Jiang, X.; Fu, J.; Zhao, J. New metallic carbon: Three dimensionally carbon allotropes comprising ultrathin diamond nanostripes. *Carbon* **2018**, *126*, 601–610. [CrossRef]
15. Moss, S. Less is more: A holey grail of materials science. *MRS Bull.* **2013**, *38*, 431–432. [CrossRef]
16. Xu, H.; Li, Y.; Wang, R. Pore-rich iron-nitrogen-doped carbon nanofoam as an efficient catalyst towards the oxygen reduction reaction. *Int. J. Hydrogen Energy* **2019**, *44*, 26285–26295. [CrossRef]
17. DeBlock, R.H.; Ko, J.S.; Sassin, M.B.; Hoffmaster, A.N.; Dunn, B.S.; Rolison, D.R.; Long, J.W. Carbon nanofoam paper enables high-rate and high-capacity Na-ion storage. *Energy Storage Mater.* **2019**, *21*, 481–486. [CrossRef]
18. Rode, A.V.; Gamaly, E.G.; Christy, A.; Gerald, J.F.; Hyde, S.; Elliman, R.; Luther-Davies, B.; Veinger, A.; Androulakis, J.; Giapintzakis, J. Unconventional magnetism in all-carbon nanofoam. *Phys. Rev. B* **2004**, *70*, 54407. [CrossRef]
19. Worsley, M.A.; Baumann, T.F. Carbon aerogels. In *Handbook of Sol-Gel Science and Technology*; Springer: Berlin/Heidelberg, Germany, 2016; pp. 1–36.
20. Georgakilas, V.; Perman, J.A.; Tucek, J.; Zboril, R. Broad family of carbon nanoallotropes: Classification, chemistry, and applications of fullerenes, carbon dots, nanotubes, graphene, nanodiamonds, and combined superstructures. *Chem. Rev.* **2015**, *115*, 4744–4822. [CrossRef]
21. Chandrasekaran, S.; Campbell, P.G.; Baumann, T.F.; Worsley, M.A. Carbon aerogel evolution: Allotrope, graphene-inspired, and 3D-printed aerogels. *J. Mater. Res.* **2017**, *32*, 4166–4185. [CrossRef]
22. Tuček, J.; Błoński, P.; Ugolotti, J.; Swain, A.K.; Enoki, T.; Zbořil, R. Emerging chemical strategies for imprinting magnetism in graphene and related 2D materials for spintronic biomedical applications. *Chem. Soc. Rev.* **2018**, *47*, 3899–3990. [CrossRef]
23. Ni, W.; Wu, H.B.; Wang, B.; Xu, R.; Lou, X.W. One-Pot Synthesis of Ultra-Light Nickel Nanofoams Composed of Nanowires and Their Transformation into Various Functional Nanofoams. *Small* **2012**, *8*, 3432–3437. [CrossRef] [PubMed]
24. Reddy, B.N.; Gupta, B.; Gacche, R. An arsenal for 21st century noxious diseases: Carbon nanomaterials. *Int. J. Nanotechnol. Appl.* **2009**, *3*, 61–76.
25. Kohno, H.; Tatsutani, K.; Ichikawa, S. Carbon nanofoam formed by laser ablation. *J. Nanosci. Nanotechnol.* **2012**, *12*, 2844–2848. [CrossRef]
26. Ju, Z.; Zhang, S.; Xing, Z.; Zhuang, Q.; Qiang, Y.; Qian, Y. Direct synthesis of few-layer F-doped graphene foam and its lithium/potassium storage properties. *ACS Appl. Mater. Interfaces* **2016**, *8*, 20682–20690. [CrossRef] [PubMed]
27. Li, C.; Li, Z.; Ye, X.; Yang, X.; Zhang, G.; Li, Z. Crosslinking-induced spontaneous growth: A novel strategy for synthesizing sandwich-type graphene@ Fe_3O_4 dots/amorphous carbon with high lithium storage performance. *Chem. Eng. J.* **2018**, *334*, 1614–1620. [CrossRef]

28. Dutta, S.; Kim, J.; Ide, Y.; Kim, J.H.; Hossain, M.S.A.; Bando, Y.; Yamauchi, Y.; Wu, K.C.-W. 3D network of cellulose-based energy storage devices and related emerging applications. *Mater. Horiz.* **2017**, *4*, 522–545. [CrossRef]
29. Błaszczyński, T.; Ślosarczyk, A.; Morawski, M. Synthesis of silica aerogel by supercritical drying method. *Procedia Eng.* **2013**, *57*, 200–206. [CrossRef]
30. Mujeebu, M.A.; Ashraf, N.; Alsuwayigh, A.H. Effect of nano vacuum insulation panel and nanogel glazing on the energy performance of office building. *Appl. Energy* **2016**, *173*, 141–151. [CrossRef]
31. Berardi, U. The development of a monolithic aerogel glazed window for an energy retrofitting project. *Appl. Energy* **2015**, *154*, 603–615. [CrossRef]
32. Song, S.H.; Park, K.H.; Kim, B.H.; Choi, Y.W.; Jun, G.H.; Lee, D.J.; Kong, B.S.; Paik, K.W.; Jeon, S. Enhanced thermal conductivity of epoxy–graphene composites by using non-oxidized graphene flakes with non-covalent functionalization. *Adv. Mater.* **2013**, *25*, 732–737. [CrossRef]
33. Zhao, S.; Yan, Y.; Gao, A.; Zhao, S.; Cui, J.; Zhang, G. Flexible polydimethylsilane nanocomposites enhanced with a three-dimensional graphene/carbon nanotube bicontinuous framework for high-performance electromagnetic interference shielding. *ACS Appl. Mater. Interfaces* **2018**, *10*, 26723–26732. [CrossRef] [PubMed]
34. Bor, J.; Lafond, O.; Merlet, H.; Le Bars, P.; Himdi, M. Technological process to control the foam dielectric constant application to microwave components and antennas. *IEEE Trans. Compon. Packag. Manuf. Technol.* **2014**, *4*, 938–942. [CrossRef]
35. Yuan, X.; Chung, T.M. Cross-linking effect on dielectric properties of polypropylene thin films and applications in electric energy storage. *Appl. Phys. Lett.* **2011**, *98*, 062901. [CrossRef]
36. Zhao, B.; Hamidinejad, M.; Zhao, C.; Li, R.; Wang, S.; Kazemi, Y.; Park, C.B. A versatile foaming platform to fabricate polymer/carbon composites with high dielectric permittivity and ultra-low dielectric loss. *J. Mater. Chem. A* **2019**, *7*, 133–140. [CrossRef]
37. Wang, G.; Liao, X.; Yang, J.; Tang, W.; Zhang, Y.; Jiang, Q.; Li, G. Frequency-selective and tunable electromagnetic shielding effectiveness via the sandwich structure of silicone rubber/graphene composite. *Compos. Sci. Technol.* **2019**, *184*, 107847. [CrossRef]
38. Molle, A.; Goldberger, J.; Houssa, M.; Xu, Y.; Zhang, S.-C.; Akinwande, D. Buckled two-dimensional Xene sheets. *Nat. Mater.* **2017**, *16*, 163. [CrossRef]
39. Geng, D.; Wu, B.; Guo, Y.; Huang, L.; Xue, Y.; Chen, J.; Yu, G.; Jiang, L.; Hu, W.; Liu, Y. Uniform hexagonal graphene flakes and films grown on liquid copper surface. *Proc. Natl. Acad. Sci. USA* **2012**, *109*, 7992–7996. [CrossRef]
40. Pashangpour, M.; Bagheri, Z.; Ghaffari, V. A comparison of electronic transport properties of graphene with hexagonal boron nitride substrate and graphane, a first principle study. *Eur. Phys. J. B* **2013**, *86*, 269. [CrossRef]
41. Butler, S.Z.; Hollen, S.M.; Cao, L.; Cui, Y.; Gupta, J.A.; Gutiérrez, H.R.; Heinz, T.F.; Hong, S.S.; Huang, J.; Ismach, A.F. Progress, challenges, and opportunities in two-dimensional materials beyond graphene. *ACS Nano* **2013**, *7*, 2898–2926. [CrossRef]
42. Bozzi, M.; Pierantoni, L.; Bellucci, S. Applications of graphene at microwave frequencies. *Radioengineering* **2015**, *24*, 661–669. [CrossRef]
43. Yuchang, Q.; Qinlong, W.; Fa, L.; Wancheng, Z. Temperature dependence of the electromagnetic properties of graphene nanosheet reinforced alumina ceramics in the X-band. *J. Mater. Chem. C* **2016**, *4*, 4853–4862. [CrossRef]
44. Jiang, W.; Xin, H.; Li, W. Microcellular 3D graphene foam via chemical vapor deposition of electroless plated nickel foam templates. *Mater. Lett.* **2016**, *162*, 105–109. [CrossRef]
45. Wang, D.; Gao, H.; Roze, E.; Qu, K.; Liu, W.; Shao, Y.; Xin, S.; Wang, Y. Synthesis and photoluminescence of three-dimensional europium-complexed graphene macroassembly. *J. Mater. Chem. C* **2013**, *1*, 5772–5778. [CrossRef]
46. Xie, X.; Zhou, Y.; Bi, H.; Yin, K.; Wan, S.; Sun, L. Large-range control of the microstructures and properties of three-dimensional porous graphene. *Sci. Rep.* **2013**, *3*, 2117. [CrossRef] [PubMed]
47. Kawai, S.; Foster, A.S.; Björkman, T.; Nowakowska, S.; Björk, J.; Canova, F.F.; Gade, L.H.; Jung, T.A.; Meyer, E. Van der Waals interactions and the limits of isolated atom models at interfaces. *Nat. Commun.* **2016**, *7*, 11559. [CrossRef] [PubMed]
48. Jiang, L.; Fan, Z. Design of advanced porous graphene materials: From graphene nanomesh to 3D architectures. *Nanoscale* **2014**, *6*, 1922–1945. [CrossRef]
49. Chowdhury, S.; Balasubramanian, R. Three-dimensional graphene-based macrostructures for sustainable energy applications and climate change mitigation. *Prog. Mater. Sci.* **2017**, *90*, 224–275. [CrossRef]
50. Sheng, H.; Wei, M.; D'Aloia, A.; Wu, G. Heteroatom polymer-derived 3D high-surface-area and mesoporous graphene sheet-like carbon for supercapacitors. *ACS Appl. Mater. Interfaces* **2016**, *8*, 30212–30224. [CrossRef]
51. Cong, H.-P.; Chen, J.-F.; Yu, S.-H. Graphene-based macroscopic assemblies and architectures: An emerging material system. *Chem. Soc. Rev.* **2014**, *43*, 7295–7325. [CrossRef]
52. Fang, Q.; Shen, Y.; Chen, B. Synthesis, decoration and properties of three-dimensional graphene-based macrostructures: A review. *Chem. Eng. J.* **2015**, *264*, 753–771. [CrossRef]
53. Chabot, V.; Higgins, D.; Yu, A.; Xiao, X.; Chen, Z.; Zhang, J. A review of graphene and graphene oxide sponge: Material synthesis and applications to energy and the environment. *Energy Environ. Sci.* **2014**, *7*, 1564–1596. [CrossRef]
54. Xia, X.; Chao, D.; Zhang, Y.Q.; Shen, Z.X.; Fan, H.J. Three-dimensional graphene and their integrated electrodes. *Nano Today* **2014**, *9*, 785–807. [CrossRef]

55. Deng, X.; Li, J.; Zhu, S.; He, F.; He, C.; Liu, E.; Shi, C.; Li, Q.; Zhao, N. Metal–organic frameworks-derived honeycomb-like Co_3O_4/three-dimensional graphene networks/Ni foam hybrid as a binder-free electrode for supercapacitors. *J. Alloys Compd.* **2017**, *693*, 16–24. [CrossRef]
56. Banciu, C.A.; Nastase, F.; Istrate, A.-I.; Veca, L.M. 3D Graphene Foam by Chemical Vapor Deposition: Synthesis, Properties, and Energy-Related Applications. *Molecules* **2022**, *27*, 3634. [CrossRef] [PubMed]
57. Ma, Y.; Chen, Y. Three-dimensional graphene networks: Synthesis, properties and applications. *Natl. Sci. Rev.* **2015**, *2*, 40–53. [CrossRef]
58. Sai, H.; Xing, L.; Xiang, J.; Cui, L.; Jiao, J.; Zhao, C.; Li, Z.; Li, F.; Zhang, T. Flexible aerogels with interpenetrating network structure of bacterial cellulose–silica composite from sodium silicate precursor via freeze drying process. *RSC Adv.* **2014**, *4*, 30453–30461. [CrossRef]
59. Thomas, T.; Agarwal, A. A facile and scalable approach in the fabrication of tailored 3D graphene foam via freeze drying. *Materials* **2021**, *14*, 864. [CrossRef]
60. Qu, B.; Lian, X.-B.; Wu, Q.-H. Growth of three-dimensional graphene films on the Ni foil. *Surf. Eng.* **2016**, *32*, 750–754. [CrossRef]
61. Hu, C.; Mou, Z.; Lu, G.; Chen, N.; Dong, Z.; Hu, M.; Qu, L. 3D graphene–Fe_3O_4 nanocomposites with high-performance microwave absorption. *Phys. Chem. Chem. Phys.* **2013**, *15*, 13038–13043. [CrossRef]
62. Zhang, Y.; Cui, W.; An, W.; Liu, L.; Liang, Y.; Zhu, Y. Combination of photoelectrocatalysis and adsorption for removal of bisphenol A over TiO_2-graphene hydrogel with 3D network structure. *Appl. Catal. B Environ.* **2018**, *221*, 36–46. [CrossRef]
63. Yang, Q.; Lu, R.; Ren, S.; Chen, C.; Chen, Z.; Yang, X. Three dimensional reduced graphene oxide/ZIF-67 aerogel: Effective removal cationic and anionic dyes from water. *Chem. Eng. J.* **2018**, *348*, 202–211. [CrossRef]
64. Wan, W.; Li, L.; Zhao, Z.; Hu, H.; Hao, X.; Winkler, D.A.; Xi, L.; Hughes, T.C.; Qiu, J. Ultrafast fabrication of covalently cross-linked multifunctional graphene oxide monoliths. *Adv. Funct. Mater.* **2014**, *24*, 4915–4921. [CrossRef]
65. Pan, H.; Zhu, S.; Mao, L. Graphene nanoarchitectonics: Approaching the excellent properties of graphene from microscale to macroscale. *J. Inorg. Organomet. Polym. Mater.* **2015**, *25*, 179–188. [CrossRef]
66. Liu, S.; Bastola, A.K.; Li, L. A 3D printable and mechanically robust hydrogel based on alginate and graphene oxide. *ACS Appl. Mater. Interfaces* **2017**, *9*, 41473–41481. [CrossRef]
67. Lv, P.; Tan, X.-W.; Yu, K.-H.; Zheng, R.-L.; Zheng, J.-J.; Wei, W. Super-elastic graphene/carbon nanotube aerogel: A novel thermal interface material with highly thermal transport properties. *Carbon* **2016**, *99*, 222–228. [CrossRef]
68. Min, B.H.; Kim, D.W.; Kim, K.H.; Choi, H.O.; Jang, S.W.; Jung, H.-T. Bulk scale growth of CVD graphene on Ni nanowire foams for a highly dense and elastic 3D conducting electrode. *Carbon* **2014**, *80*, 446–452. [CrossRef]
69. Yang, Z.; Chabi, S.; Xia, Y.; Zhu, Y. Preparation of 3D graphene-based architectures and their applications in supercapacitors. *Prog. Nat. Sci. Mater. Int.* **2015**, *25*, 554–562. [CrossRef]
70. Xu, L.; Wei, N.; Zheng, Y.; Fan, Z.; Wang, H.-Q.; Zheng, J.-C. Graphene-nanotube 3D networks: Intriguing thermal and mechanical properties. *J. Mater. Chem.* **2012**, *22*, 1435–1444. [CrossRef]
71. Thomas, T.; Zhang, C.; Feliciano Ruiz, K.M.; Ramos-Pagan, C.I.; Negron, D.M.R.; Boesl, B.; Agarwal, A. Engineering Graphene-Ceramic 3D Composite Foams by Freeze Drying. *Adv. Eng. Mater.* **2021**, *23*, 2001546. [CrossRef]
72. Ming, R.; Ding, Y.; Chang, F.; He, X.; Feng, J.; Wang, C.; Zhang, P. Humidity-dependant compression properties of graphene oxide foams prepared by freeze-drying technique. *Micro Nano Lett.* **2013**, *8*, 66–67. [CrossRef]
73. Zhou, W.; Wang, Z.L. Three-dimensional nanoarchitectures. In *Designing Next-Generation Devices*; Springer Science Business Media, LLC: New York, NY, USA, 2011.
74. Fan, X.; Chen, X.; Dai, L. 3D graphene based materials for energy storage. *Curr. Opin. Colloid Interface Sci.* **2015**, *20*, 429–438. [CrossRef]
75. Yao, H.; Zhang, G.; Zhang, F.; Li, W.; Yang, Y.; Chen, L. A novel Ni Coordination Supramolecular Network hybrid monolith of 3D graphene as electrode materials for supercapacitors. *Mater. Today Energy* **2017**, *6*, 164–172. [CrossRef]
76. Tang, W.; Peng, L.; Yuan, C.; Wang, J.; Mo, S.; Zhao, C.; Yu, Y.; Min, Y.; Epstein, A.J. Facile synthesis of 3D reduced graphene oxide and its polyaniline composite for super capacitor application. *Synth. Met.* **2015**, *202*, 140–146. [CrossRef]
77. Wang, K.; Wang, W.; Wang, H.; Liu, L.; Xu, Z.; Fu, H.; Zhao, L.; Zhang, X.; Chen, L.; Zhao, Y. 3D graphene foams/epoxy composites with double-sided binder polyaniline interlayers for maintaining excellent electrical conductivities and mechanical properties. *Compos. Part A Appl. Sci. Manuf.* **2018**, *110*, 246–257. [CrossRef]
78. Li, H.; Liu, L.; Yang, F. Covalent assembly of 3D graphene/polypyrrole foams for oil spill cleanup. *J. Mater. Chem. A* **2013**, *1*, 3446–3453. [CrossRef]
79. Wang, H.; Yuan, X.; Zeng, G.; Wu, Y.; Liu, Y.; Jiang, Q.; Gu, S. Three dimensional graphene based materials: Synthesis and applications from energy storage and conversion to electrochemical sensor and environmental remediation. *Adv. Colloid Interface Sci.* **2015**, *221*, 41–59. [CrossRef]
80. Asen, P.; Shahrokhian, S. A high performance supercapacitor based on graphene/polypyrrole/Cu_2O–$Cu(OH)_2$ ternary nanocomposite coated on nickel foam. *J. Phys. Chem. C* **2017**, *121*, 6508–6519. [CrossRef]
81. Salvatierra, R.V.; Cava, C.E.; Roman, L.S.; Oliveira, M.M.; Zarbin, A.J. The total chemical synthesis of polymer/graphene nanocomposite films. *Chem. Commun.* **2016**, *52*, 1629–1632. [CrossRef]
82. Wang, Y.Q.; Liu, Y.F. Free vibration and buckling of polymeric shells reinforced with 3D graphene foams. *Results Phys.* **2019**, *14*, 102510. [CrossRef]

83. Jia, J.; Sun, X.; Lin, X.; Shen, X.; Mai, Y.-W.; Kim, J.-K. Exceptional electrical conductivity and fracture resistance of 3D interconnected graphene foam/epoxy composites. *ACS Nano* **2014**, *8*, 5774–5783. [CrossRef] [PubMed]
84. Ormategui, N.; Veloso, A.; Leal, G.P.; Rodriguez-Couto, S.; Tomovska, R. Design of stable and powerful nanobiocatalysts, based on enzyme laccase immobilized on self-assembled 3D graphene/polymer composite hydrogels. *ACS Appl. Mater. Interfaces* **2015**, *7*, 14104–14112. [CrossRef] [PubMed]
85. Rinaldi, A.; Tamburrano, A.; Fortunato, M.; Sarto, M. A flexible and highly sensitive pressure sensor based on a PDMS foam coated with graphene nanoplatelets. *Sensors* **2016**, *16*, 2148. [CrossRef] [PubMed]
86. Zhao, Y.-H.; Wu, Z.-K.; Bai, S.-L. Study on thermal properties of graphene foam/graphene sheets filled polymer composites. *Compos. Part A Appl. Sci. Manuf.* **2015**, *72*, 200–206. [CrossRef]
87. Jun, Y.-S.; Sy, S.; Ahn, W.; Zarrin, H.; Rasen, L.; Tjandra, R.; Amoli, B.M.; Zhao, B.; Chiu, G.; Yu, A. Highly conductive interconnected graphene foam based polymer composite. *Carbon* **2015**, *95*, 653–658. [CrossRef]
88. Zhao, Y.-H.; Zhang, Y.-F.; Bai, S.-L.; Yuan, X.-W. Carbon fibre/graphene foam/polymer composites with enhanced mechanical and thermal properties. *Compos. Part B Eng.* **2016**, *94*, 102–108. [CrossRef]
89. Yuan, C.; Zhou, L.; Hou, L. Facile fabrication of self-supported three-dimensional porous reduced graphene oxide film for electrochemical capacitors. *Mater. Lett.* **2014**, *124*, 253–255. [CrossRef]
90. Gnanasekaran, K.; Heijmans, T.; Van Bennekom, S.; Woldhuis, H.; Wijnia, S.; de With, G.; Friedrich, H. 3D printing of CNT-and graphene-based conductive polymer nanocomposites by fused deposition modeling. *Appl. Mater. Today* **2017**, *9*, 21–28. [CrossRef]
91. Shao, L.; Shi, L.; Li, X.; Song, N.; Ding, P. Synergistic effect of BN and graphene nanosheets in 3D framework on the enhancement of thermal conductive properties of polymeric composites. *Compos. Sci. Technol.* **2016**, *135*, 83–91. [CrossRef]
92. Loeblein, M.; Jing, L.; Liu, M.; Cheah, J.; Tsang, S.; Teo, E. A "hairy" polymer/3D-foam hybrid for flexible high performance thermal gap filling applications in harsh environments. *RSC Adv.* **2017**, *7*, 39292–39298. [CrossRef]
93. Niyobuhungiro, D.; Hong, L. Graphene Polymer Composites: Art of Review on Fabrication Method, Properties, and Future Perspectives. Advances in Science and Technology. *Res. J.* **2021**, *15*, 37–49.
94. Idowu, A.; Boesl, B.; Agarwal, A. 3D graphene foam-reinforced polymer composites—A review. *Carbon* **2018**, *135*, 52–71. [CrossRef]
95. Wu, Y.; Wang, Z.; Liu, X.; Shen, X.; Zheng, Q.; Xue, Q.; Kim, J.-K. Ultralight graphene foam/conductive polymer composites for exceptional electromagnetic interference shielding. *ACS Appl. Mater. Interfaces* **2017**, *9*, 9059–9069. [CrossRef]
96. Eswaraiah, V.; Sankaranarayanan, V.; Ramaprabhu, S. Functionalized graphene–PVDF foam composites for EMI shielding. *Macromol. Mater. Eng.* **2011**, *296*, 894–898. [CrossRef]
97. Hu, Z.; Ji, X.; Li, B.; Luo, Y. A self-assembled graphene/polyurethane sponge for excellent electromagnetic interference shielding performance. *RSC Adv.* **2019**, *9*, 25829–25835. [CrossRef]
98. Lee, J.-S.; Ahn, H.-J.; Yoon, J.-C.; Jang, J.-H. Three-dimensional nano-foam of few-layer graphene grown by CVD for DSSC. *Phys. Chem. Chem. Phys.* **2012**, *14*, 7938–7943. [CrossRef]
99. Tang, B.; Hu, G.; Gao, H.; Shi, Z. Three-dimensional graphene network assisted high performance dye sensitized solar cells. *J. Power Sources* **2013**, *234*, 60–68. [CrossRef]
100. Ye, S.; Feng, J. Self-assembled three-dimensional hierarchical graphene/polypyrrole nanotube hybrid aerogel and its application for supercapacitors. *ACS Appl. Mater. Interfaces* **2014**, *6*, 9671–9679. [CrossRef]
101. Yu, M.; Ma, Y.; Liu, J.; Li, S. Polyaniline nanocone arrays synthesized on three-dimensional graphene network by electrodeposition for supercapacitor electrodes. *Carbon* **2015**, *87*, 98–105. [CrossRef]
102. Sim, Y.; Kwak, J.; Kim, S.-Y.; Jo, Y.; Kim, S.; Kim, S.Y.; Kim, J.H.; Lee, C.-S.; Jo, J.H.; Kwon, S.-Y. Formation of 3D graphene–Ni foam heterostructures with enhanced performance and durability for bipolar plates in a polymer electrolyte membrane fuel cell. *J. Mater. Chem. A* **2018**, *6*, 1504–1512. [CrossRef]
103. He, J.; Han, M.; Wen, K.; Liu, C.; Zhang, W.; Liu, Y.; Su, X.; Zhang, C.; Liang, C. Absorption-dominated electromagnetic interference shielding assembled composites based on modular design with infrared camouflage and response switching. *Compos. Sci. Technol.* **2023**, *231*, 109799. [CrossRef]
104. Kausar, A. Advances in polymer-anchored carbon nanotube foam: A review. *Polym. -Plast. Technol. Mater.* **2019**, *58*, 1965–1978. [CrossRef]
105. Li, Y.; Huang, X.; Zeng, L.; Li, R.; Tian, H.; Fu, X.; Wang, Y.; Zhong, W.-H. A review of the electrical and mechanical properties of carbon nanofiller-reinforced polymer composites. *J. Mater. Sci.* **2019**, *54*, 1036–1076. [CrossRef]
106. Sudhakar, K.; Reddy, N.N.; Jayaramudu, T.; Jayaramudu, J.; Reddy, A.B.; Manjula, B.; Sadiku, E.R. *Aerogels and Foamed Nanostructured Polymer Blends: Design and Applications of Nanostructured Polymer Blends and Nanocomposite Systems*; Elsevier: Amsterdam, The Netherlands, 2016; pp. 75–99.
107. Chen, Z.; Xu, C.; Ma, C.; Ren, W.; Cheng, H.M. Lightweight and flexible graphene foam composites for high-performance electromagnetic interference shielding. *Adv. Mater.* **2013**, *25*, 1296–1300. [CrossRef]
108. Yu, W.-C.; Zhang, G.-Q.; Liu, Y.-H.; Xu, L.; Yan, D.-X.; Huang, H.-D.; Tang, J.-H.; Xu, J.-Z.; Li, Z.-M. Selective electromagnetic interference shielding performance and superior mechanical strength of conductive polymer composites with oriented segregated conductive networks. *Chem. Eng. J.* **2019**, *373*, 556–564. [CrossRef]

109. Shen, B.; Li, Y.; Zhai, W.; Zheng, W. Compressible graphene-coated polymer foams with ultralow density for adjustable electromagnetic interference (EMI) shielding. *ACS Appl. Mater. Interfaces* **2016**, *8*, 8050–8057. [CrossRef]
110. Wang, H.; Sun, K.; Tao, F.; Stacchiola, D.J.; Hu, Y.H. 3D honeycomb-like structured graphene and its high efficiency as a counter-electrode catalyst for dye-sensitized solar cells. *Angew. Chem. Int. Ed.* **2013**, *52*, 9210–9214. [CrossRef]
111. Li, D.; Zhong, H. Facile engineering 3-D photothermal laser induced graphene for efficient steam generation. *Sol. Energy Mater. Sol. Cells* **2023**, *250*, 112104. [CrossRef]
112. Miah, M.; Hota, P.; Mondal, T.K.; Chen, R.; Saha, S.K. Mixed metal sulfides ($FeNiS_2$) nanosheets decorated reduced graphene oxide for efficient electrode materials for supercapacitors. *J. Alloys Compd.* **2023**, *933*, 167648. [CrossRef]
113. El-Kady, M.F.; Shao, Y.; Kaner, R.B. Graphene for batteries, supercapacitors and beyond. *Nat. Rev. Mater.* **2016**, *1*, 16033. [CrossRef]
114. Kumar, R.; Sahoo, S.; Joanni, E.; Singh, R.K. A review on the current research on microwave processing techniques applied to graphene-based supercapacitor electrodes: An emerging approach beyond conventional heating. *J. Energy Chem.* **2022**, *74*, 252–282. [CrossRef]
115. Gao, Y. Graphene and polymer composites for supercapacitor applications: A review. *Nanoscale Res. Lett.* **2017**, *12*, 387. [CrossRef]
116. Manjakkal, L.; Núñez, C.G.; Dang, W.; Dahiya, R. Flexible self-charging supercapacitor based on graphene-Ag-3D graphene foam electrodes. *Nano Energy* **2018**, *51*, 604–612. [CrossRef]
117. Zhao, Y.; Liu, J.; Hu, Y.; Cheng, H.; Hu, C.; Jiang, C.; Jiang, L.; Cao, A.; Qu, L. Highly compression-tolerant supercapacitor based on polypyrrole-mediated graphene foam electrodes. *Adv. Mater.* **2013**, *25*, 591–595. [CrossRef]
118. Yang, X.; Fan, S.; Li, Y.; Guo, Y.; Li, Y.; Ruan, K.; Zhang, S.; Zhang, J.; Kong, J.; Gu, J. Synchronously improved electromagnetic interference shielding and thermal conductivity for epoxy nanocomposites by constructing 3D copper nanowires/thermally annealed graphene aerogel framework. *Compos. Part A Appl. Sci. Manuf.* **2020**, *128*, 105670. [CrossRef]
119. Ni, J.; Zhan, R.; Qiu, J. Constructing honeycomb conductive rings in graphene foam/epoxy resin metacomposites for adjustable negative permittivity, low dielectric loss tangent and mechanical enhancement. *Org. Electron.* **2020**, *82*, 105706. [CrossRef]
120. Mehtab, T.; Yasin, G.; Arif, M.; Shakeel, M.; Korai, R.M.; Nadeem, M.; Muhammad, N.; Lu, X. Metal-organic frameworks for energy storage devices: Batteries and supercapacitors. *J. Energy Storage* **2019**, *21*, 632–646. [CrossRef]
121. Yang, F.; Xu, M.; Bao, S.-J.; Wei, H.; Chai, H. Self-assembled hierarchical graphene/polyaniline hybrid aerogels for electrochemical capacitive energy storage. *Electrochim. Acta* **2014**, *137*, 381–387. [CrossRef]
122. Kamyshny, A.; Magdassi, S. Conductive nanomaterials for 2D and 3D printed flexible electronics. *Chem. Soc. Rev.* **2019**, *48*, 1712–1740. [CrossRef]
123. Mahmood, N.; Zhang, C.; Yin, H.; Hou, Y. Graphene-based nanocomposites for energy storage and conversion in lithium batteries, supercapacitors and fuel cells. *J. Mater. Chem. A* **2014**, *2*, 15–32. [CrossRef]
124. Chen, S.-Y.; Chung, S.-H. Advanced current collectors with carbon nanofoams for electrochemically stable lithium—Sulfur cells. *Nanomaterials* **2021**, *11*, 2083. [CrossRef]
125. Hwang, J.; Kim, S.-I.; Yoon, J.-C.; Ha, S.-J.; Jang, J.-H. Realizing battery-like energy density with asymmetric supercapacitors achieved by using highly conductive three-dimensional graphene current collectors. *J. Mater. Chem. A* **2017**, *5*, 13347–13356. [CrossRef]
126. Muñoz, E.; Soto-Garrido, R. Analytic approach to magneto-strain tuning of electronic transport through a graphene nanobubble: Perspectives for a strain sensor. *J. Phys. Condens. Matter* **2017**, *29*, 445302. [CrossRef]
127. Song, T.; Myoung, N.; Lee, H.; Park, H.C. Machine learning approach to the recognition of nanobubbles in graphene. *Appl. Phys. Lett.* **2021**, *119*, 193103. [CrossRef]
128. Si, C.; Sun, Z.; Liu, F. Strain engineering of graphene: A review. *Nanoscale* **2016**, *8*, 3207–3217. [CrossRef]
129. Su, H.; Hu, Y.H. Recent advances in graphene-based materials for fuel cell applications. *Energy Sci. Eng.* **2021**, *9*, 958–983. [CrossRef]
130. Mahyari, M.; Laeini, M.S.; Shaabani, A. Aqueous aerobic oxidation of alkyl arenes and alcohols catalyzed by copper (II) phthalocyanine supported on three-dimensional nitrogen-doped graphene at room temperature. *Chem. Commun.* **2014**, *50*, 7855–7857. [CrossRef]
131. Lotfi, N.; Shahrabi, T.; Yaghoubinezhad, Y.; Darband, G.B. Direct electrodeposition of platinum nanoparticles@ graphene oxide@ nickel-copper@ nickel foam electrode as a durable and cost-effective catalyst with remarkable performance for electrochemical hydrogen evolution reaction. *Appl. Surf. Sci.* **2020**, *505*, 144571. [CrossRef]
132. Simakov, D.S. *Renewable Synthetic Fuels and Chemicals from Carbon Dioxide: Fundamentals, Catalysis, Design Considerations and Technological Challenges*; Springer: Berlin/Heidelberg, Germany, 2017.
133. Hornés, A.; Pesce, A.; Hernández-Afonso, L.; Morata, A.; Torrell, M.; Tarancón, A. 3D Printing of Fuel Cells and Electrolyzers. *3D Print. Energy Appl.* **2022**, 273–306.
134. Yu, D.; Goh, K.; Wang, H.; Wei, L.; Jiang, W.; Zhang, Q.; Dai, L.; Chen, Y. Scalable synthesis of hierarchically structured carbon nanotube–graphene fibres for capacitive energy storage. *Nat. Nanotechnol.* **2014**, *9*, 555. [CrossRef]
135. Xu, T.; Ding, Y.; Wang, Z.; Zhao, Y.; Wu, W.; Fong, H.; Zhu, Z. Three-dimensional and ultralight sponges with tunable conductivity assembled from electrospun nanofibers for a highly sensitive tactile pressure sensor. *J. Mater. Chem. C* **2017**, *5*, 10288–10294. [CrossRef]
136. Navarro-Pardo, F.; Martinez-Hernandez, A.L.; Velasco-Santos, C. Carbon nanotube and graphene based polyamide electrospun nanocomposites: A review. *J. Nanomater.* **2016**, *2016*, 14. [CrossRef]

137. Kwon, S.R.; Harris, J.; Zhou, T.; Loufakis, D.; Boyd, J.G.; Lutkenhaus, J.L. Mechanically strong graphene/aramid nanofiber composite electrodes for structural energy and power. *ACS Nano* **2017**, *11*, 6682–6690. [CrossRef]
138. Rout, S.; Qi, Z.; Petrosyan, L.S.; Shahbazyan, T.V.; Biener, M.M.; Bonner, C.E.; Noginov, M.A. Effect of Random Nanostructured Metallic Environments on Spontaneous Emission of HITC Dye. *Nanomaterials* **2020**, *10*, 2135. [CrossRef]
139. Ebrahimi, M.; Botelho, M.; Lu, W.; Monmaturapoj, N. Integrated approach in designing biphasic nanocomposite collagen/nBCP scaffolds with controlled porosity and permeability for bone tissue engineering. *J. Biomed. Mater. Res. Part B Appl. Biomater.* **2020**, *108*, 1738–1753. [CrossRef]